Gene Expression, Vol. 19, pp. 15–24
Printed in the USA.

1052-2166/19 $90.00 + .00
DOI: https://doi.org/10.3727/105221618X15320123457380
E-ISSN 1555-3884
www.cognizantcommunication.com

In *Atp7b*$^{-/-}$ Mice Modeling Wilson's Disease Liver Repopulation With Bone Marrow-Derived Myofibroblasts or Inflammatory Cells and Not Hepatocytes Is Deleterious

Yogeshwar Sharma,* Jinghua Liu,† Kathleen E. Kristian,‡ Antonia Follenzi,§¶ and Sanjeev Gupta*§#

*Department of Medicine, Albert Einstein College of Medicine, Bronx, NY, USA
†Department of Obstetrics and Gynecology, Shanghai Public Health Clinical Center, Shanghai, P.R. China
‡Department of Chemistry, Iona College, New Rochelle, NY, USA
§Department of Pathology, Albert Einstein College of Medicine, Bronx, NY, USA
¶Department of Health Sciences, Università del Piemonte Orientale "A. Avogadro", Novara, Italy
#Marion Bessin Liver Research Center, Diabetes Center, Cancer Center, and Ruth L. and David S. Gottesman Institute for Stem Cell and Regenerative Medicine Research, Albert Einstein College of Medicine, Bronx, NY, USA

In Wilson's disease, *ATP7B* mutations impair copper excretion with liver or brain damage. Healthy transplanted hepatocytes repopulate the liver, excrete copper, and reverse hepatic damage in animal models of Wilson's disease. In *Fah*$^{-/-}$ mice with tyrosinemia and -1 antitrypsin mutant mice, liver disease is resolved by expansions of healthy hepatocytes derived from transplanted healthy bone marrow stem cells. This potential of stem cells has not been defined for Wilson's disease. In diseased *Atp7b*$^{-/-}$ mice, we reconstituted bone marrow with donor cells expressing green fluorescent protein reporter from healthy transgenic mice. Mature hepatocytes originating from donor bone marrow were identified by immunostaining for green fluorescence protein and bile canalicular marker, dipeptidylpeptidase-4. Mesenchymal and inflammatory cell markers were used for other cells from donor bone marrow cells. Gene expression, liver tests, and tissues were analyzed for outcomes in *Atp7b*$^{-/-}$ mice. After bone marrow transplantation in *Atp7b*$^{-/-}$ mice, donor-derived hepatocytes containing bile canaliculi appeared within weeks. Despite this maturity, donor-derived hepatocytes neither divided nor expanded. The liver of *Atp7b*$^{-/-}$ mice was not repopulated by donor-derived hepatocytes: *Atp7b* mRNA remained undetectable; liver tests, copper content, and fibrosis actually worsened. Restriction of proliferation in hepatocytes accompanied oxidative DNA damage. By contrast, donor-derived mesenchymal and inflammatory cells extensively proliferated. These contributed to fibrogenesis through greater expression of inflammatory cytokines. In Wilson's disease, donor bone marrow-derived cells underwent different fates: hepatocytes failed to proliferate; inflammatory cells proliferated to worsen disease outcomes. This will help guide stem cell therapies for conditions with proinflammatory or profibrogenic microenvironments.

Key words: Copper; Cell therapy; Differentiation; Stem cells; Bone marrow transplantation

INTRODUCTION

Physiologically regulated gene expression could be restored by repopulating liver with healthy cells. This offers opportunities for therapeutics and translational models[1–6]. Liver conditions constitute multiple targets for cell therapy[7]. The potential of stem cell-derived lineages has been largely understood at gene expression levels[8,9]. This may not accurately predict whether after transplantation cells will engraft and proliferate. As mature hepatocytes possess unique structures (gap junctions and bile canaliculi)[10,11], this should allow alternative ways to determine fates of stem cells.

In *Fah*$^{-/-}$ mouse model of hereditary tyrosinemia, transplanted adult hepatocytes repopulate the liver and correct the disease[3,4]. Hepatocytes originating from donor cells after bone marrow transplantation (BMT) exerted similar outcomes[3]. Also, in mice with mutant human -1 antitrypsin, liver injury improved after intraportal transplantation of healthy BM-derived cells[12].

These stem cell therapies should be relevant for Wilson's disease (WD). Because of *ATP7B* mutations, hepatobiliary copper (Cu) excretion is deficient in WD. This causes serious liver and/or brain damage[13]. In animal models, biliary Cu excretion in WD may be restored by

Address correspondence to Sanjeev Gupta, M.D., Albert Einstein College of Medicine, Ullmann Building, Room 625, 1300 Morris Park Avenue, Bronx, NY 10461, USA. Tel: 718-430-3309; Fax: 718-430-8975; E-mail: sanjeev.gupta@einstein.yu.edu

gene therapy or by transplanting healthy hepatocytes[14–16]. For instance, in LEC rats modeling hepatic WD, transplanted healthy hepatocytes repopulated the liver with disease correction: *Atp7b* mRNA deficiency resolved, and hepatic injury and fibrosis regressed[14,15]. For transplanted hepatocytes to excrete Cu, reconstitution was necessary of bile canaliculi. This will be similarly critical for treating WD with stem cells[17].

To determine the therapeutic potential of BM-derived hepatocytes, we used hepatic Cu toxicosis model of WD in *Atp7b*$^{-/-}$ mice[18]. After intrahepatic transplantation, BM-derived nucleated cells were rapidly cleared from the liver[19]; we considered that BM reconstitution will be better. After BMT, donor-derived stem cells should constantly appear in the blood with recurrent opportunities for originating hepatocytes. In turn, these donor-derived hepatocytes should have proliferated as replacements for damaged and lost native hepatocytes.

MATERIALS AND METHODS

Animals

The Animal Care and Use Committee of Albert Einstein College of Medicine approved the protocols. Donor C57BL/6 mice were from the National Cancer Institute (Bethesda, MD); transgenic C57BL/6-TgCAG-EGFP/1Osb/J mice expressing green fluorescent protein (GFP) were from Jackson Laboratories (Bar Harbor, ME). GFP$^{+/-}$ donors were used due to neurotoxicity in GFP$^{+/+}$ mice. In GFP$^{+/-}$ mice, 50% cells expressed GFP; a correction factor of 2 was applied for donor-derived cells. *Atp7b*$^{-/-}$ mice were originally from S. Lutsenko. These were backcrossed 10 times into C57BL/6 background in stem cells, animal models, and cell therapy core. Animals received chow with 11.8 mg copper/kg (Ralston Purina, St. Louis, MO, USA).

Bone Marrow Transplant

Femur and tibia were flushed by Dulbecco's modified Eagle's medium (DMEM) containing 5% fetal bovine serum (Life Technologies, Carlsbad, CA, USA) with RBC lysis as described previously[20]. *Atp7b*$^{-/-}$ mice (6–7 weeks of age; males and females in equal numbers) received total body irradiation (TBI) to 6 and 5 Gray in two sessions 3 h apart. This was followed by 8–10 10^6 total BM cells in DMEM via the tail vein. Death was not an end point.

Hepatocyte Transplantation

Donor GFP$^+$ transgenic hepatocytes were isolated by collagenase perfusion[21]. Freshly isolated 1 10^6 hepatocytes in 0.1 ml of DMEM were transplanted into 6- to 7-week-old *Atp7b*$^{-/-}$ mice ($n = 6$) via the spleen. Animals were sacrificed for liver repopulation analysis after 1 and 3 months.

GFP$^+$ BM-Derived Cells and Hepatocytes

Tissues were fixed in 4% paraformaldehyde in phosphate-buffered saline (PAF), pH 7.4, for 4 h; immersed in 20% and 30% sucrose for 2 and 36 h, respectively; embedded in optimal cooling temperature (OCT) resin; and stored at −80°C. Five-micrometer cryosections were postfixed with PAF and stained with rabbit anti-GFP (1:300; Molecular Probes, Life Technologies), using for detection either Alexa Fluor® 488-conjugated goat anti-rabbit IgG (1:500; Cat. No. A-11008; Molecular Probes), as described previously[20], or goat anti-rabbit IgG, horseradish peroxidase conjugate (1:500; AP187P; Sigma-Aldrich, St. Louis, MO, USA) with DAB$^+$ Substrate Chromogen (Dako Inc., Carpinteria, CA). For donor-derived Kupffer cells (KCs), monocytes, or mesenchymal cells, GFP staining was followed by F4/80 staining with phycoerythrin-conjugated antibody (1:100; Cat. No. MF48004; Caltag Labs, UK) or vimentin staining with Alexa Fluor 647-conjugated antibody (1:100; Cat. No. 9856; Cell Signaling Technology, Danvers, MA, USA). For donor-derived hepatocytes, GFP staining was followed by albumin staining with phycoerythrin-conjugated anti-rabbit goat IgG (1:100; Cat. No. T6778; Sigma-Aldrich). Dipeptidylpeptidase-4 (Dpp4) was stained with fluorescein isothiocynate-conjugated antibody (1:100; Cat. No. 559652; BD Biosciences, San Diego, CA, USA). Counterstaining used Fluorishield with DAPI (Cat. No. GTX30920; GeneTex, Irvine, CA). Morphometry used multiple tissue sections from several mice ($n = 3$–4 each).

Liver Histology and Grading

Tissues were fixed in 10% buffered formalin for paraffin embedding and hematoxylin–eosin staining. Tissue grading included steatosis, polyploidy (megalocytes with enlarged nuclei containing >diploid DNA), apoptosis, and mitosis with maximal score of 13, as described previously[22].

Hepatic Fibrosis

Collagen was stained by Sirius Red (Picrosirius Red Stain Kit; Cat. No. 24901; Polysciences Inc., Warrington, PA, USA). Stained areas were quantitated under 400 magnification by ImageJ software (NCI, Bethesda, MD, USA). Hydroxyproline was measured by a kit (MAK008; Sigma-Aldrich).

Hepatic DNA Damage

Tissue sections were fixed with ethanol and treated with 250 ng/ml RNAse for 1 h at 37°C. DNA was denatured by 4 M HCl for 7 min followed by neutralization with 50 mM Tris base for 2 min. Sections were blocked with 10% goat serum in PBS for 1 h and incubated with 8-oxo-dG antibody (1:1,000; Cat. No. 4354-MC-050; Clone 2E2; Trevigen Inc., Gaithersburg, MD, USA)

overnight at room temperature. Detection used Alexa Fluor® 647-conjugated goat anti-mouse IgG (1:100; Cat. No. 4410; Cell Signaling Technology) for 1 h with DAPI counterstaining.

Hepatic Cu Content

Tissue samples, 2–5 mg in weight, were desiccated and solubilized in 10 mM nitric acid, as described previously[23]. Cu was measured by atomic absorption spectrometry with detection limit of 100 ng/g liver (Varian AA240; Varian Medical Systems, Palo Alto, CA, USA).

Reverse Transcription (RT)-PCR

Total RNA was extracted by TRIzol reagent (Invitrogen Corp., Carlsbad, CA, USA), cleaned with RNeasy, and treated with DNase (Qiagen Corp., Valencia, CA, USA). cDNA was prepared from 1 μg of RNA with Omniscript RT Kit (Qiagen Corp.). PCR cycles for *Atp7b* and *Gapdh* were as follows: denaturation at 94°C 3 min; 30 cycles at 94°C 30 s, 60°C 45 s, 72°C 45 s; and 72°C 7 min. PCR products were resolved in 2% agarose. Quantitative RT-PCR for fibrosis and inflammation-related genes used QuantiTect® SYBR® Green PCR kit (Cat. No. 204143; Qiagen Corp.) with triplicate samples per condition. PCR cycles were as follows: denaturation at 95°C 10 min; 40 cycles at 95°C 15 s, 60°C 60 s; and 72°C 10 min. Primers are listed in Table 1. Gene expression was normalized to *Gapdh*. Fold differences used the 2 Ct method.

Serological Tests

Samples were stored at −20°C. A commercial kit was used for serum alanine aminotransferase activity (ALT; Cat. No. 700260; Cayman Chemical, Ann Arbor, MI, USA). Serum ceruloplasmin was measured as described previously[14].

Statistical Analysis

Data are shown as means ± SEM. Differences were analyzed by *t*-tests or analysis of variance (ANOVA) with Kruskall–Wallis test by GraphPad Prism7 (GraphPad Software, La Jolla, CA, USA). A value of $p < 0.05$ was considered significant.

RESULTS

With BMT, no fatality was observed over 2 weeks in *Atp7b*$^{-/-}$ mice. BM chimerism was >85%, as determined in randomly selected mice ($n = 5$) by flow cytometry for GFP^{+} blood cells. This reproduced our experience with BMT protocol[20].

We established groups of healthy C57BL/6 and *Atp7b*$^{-/-}$ mice (Fig. 1A). To reveal BM-derived cells, we analyzed mice 3 months after BMT ($n = 3$) and found GFP^{+} cells (Fig. 1B). These were mostly in hepatic sinusoids (i.e., KC or monocytes). GFP^{+} hepatocytes with large nuclei, abundant cytoplasm, and albumin were infrequent (0–1 per section). Donor-derived hepatocytes displayed Dpp4^{+} bile canaliculi. When adult hepatocytes were transplanted, cells engrafted next to portal areas. After 1 month, 2 ± 3 transplanted hepatocytes were in each group. Transplanted hepatocytes after 3 months constituted larger groups (35 ± 28 cells each, $p < 0.001$). Thus, in *Atp7b*$^{-/-}$ mice, healthy hepatocytes proliferated.

In untreated *Atp7b*$^{-/-}$ controls ($n = 40$), 3 mice (7%) died spontaneously over 12 months. In *Atp7b*$^{-/-}$ mice plus BMT ($n = 53$), 27 mice (51%) died over 12 months ($p < 0.001$). No mortality was observed in healthy C57BL/6 mice.

Table 1. RT-PCR Primers

Gene (NCBI ID)	Primers	Amplicon Size	T_m (°C)
Tgfβ1 (21803)	Forward: 5 -CTCCCGTGGCTTCTAGTGC-3 Reverse: 5 -GCCTTAGTTTGGACAGGATCTG-3	133	60
Collagen type 1 (12842)	Forward: 5 -GCTCCTCTTAGGGGCCACT-3 Reverse: 5 -CCACGTCTCACCATTGGGG-3	103	60
Timp1 (21857)	Forward: 5 -CGAGACCACCTTATACCAGCG-3 Reverse: 5 -ATGACTGGGGTGTAGGCGTA-3	108	60
Mmp2 (17390)	Forward: 5 -ACCTGAACACTTTCTATGGCTG-3 Reverse: 5 -CTTCCGCATGGTCTCGATG-3	140	60
Tnf (21926)	Forward: 5 -CAGGCGGTGCCTATGTCTC-3 Reverse: 5 -CGATCACCCCGAAGTTCAGTAG-3	89	60
Il6 (16193)	Forward: 5 -TCTATACCACTTCACAAGTCGGA-3 Reverse: 5 -GAATTGCCATTGCACAACTCTTT-3	88	60
Atp7b (11979)	Forward: 5 -GGGGACGATGCCTGAACAG-3 Reverse, 5 -TAGCCAACATTGTCGAAGGCG-3	135	60
Gapdh (2597)	Forward: 5 -GGCCTCCAAGGAGTAAGACC-3 Reverse: 5 -AGGGGTCTACATGGCAACTG-3	127	60

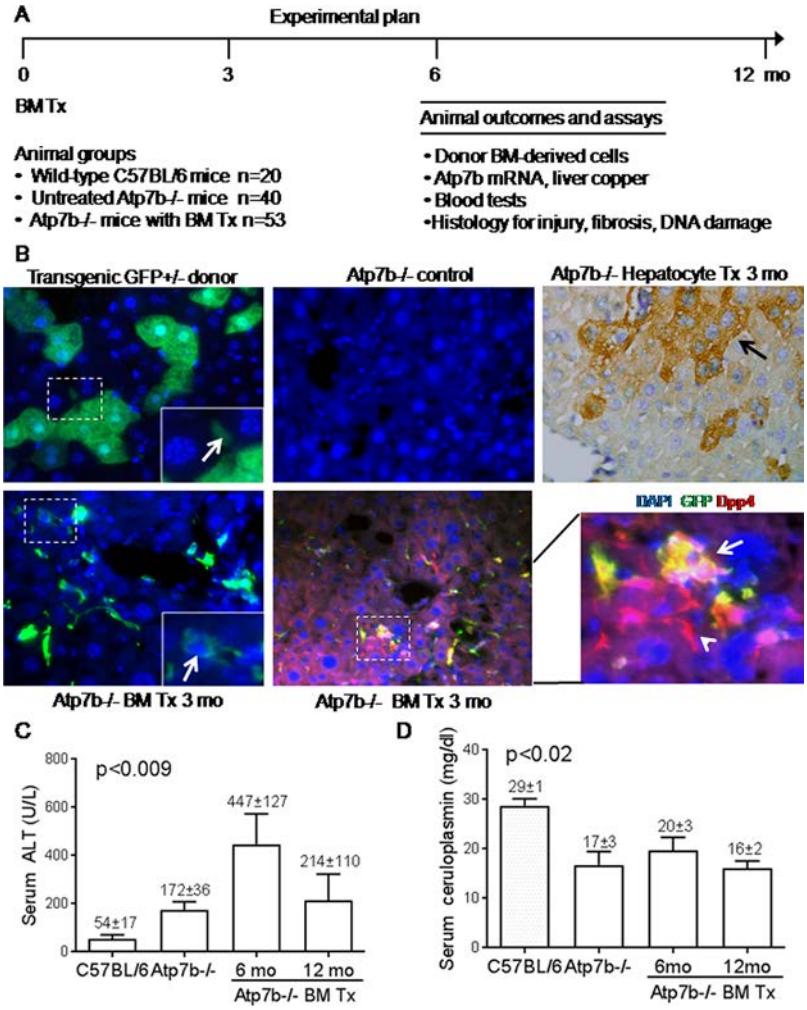

Figure 1. Animal outcomes after bone marrow transplantation (BMT). (A) Experimental plan and timeline, including animal groups and end points over the 12-month study period. (B) Green fluorescent protein (GFP) expression in hepatocytes and other cell types in donor liver (top left; inset: GFP^+ cell in hepatic sinusoid, arrow). GFP was absent in C57BL/6 or *Atp7b*$^{-/-}$ controls (top middle). Transplanted GFP^+ hepatocytes after 3 months in *Atp7b*$^{-/-}$ mice forming expanding cluster (arrow, top right, DAB color development). GFP^+ donor-derived cells in *Atp7b*$^{-/-}$ mice 3 months after BMT (inset at bottom left: arrow, GFP^+ hepatocyte). GFP and bile canalicular Dpp4 (red) in *Atp7b*$^{-/-}$ mouse 3 months after BMT (magnified view of boxed area: arrow, $GFP^+/Dpp4^+$ hepatocyte; arrowhead, $Dpp4^+$ sinusoidal cell). Original magnification: 600 (top), 400 (bottom). DAPI counterstain. (C) Serum alanine aminotransferase activity (ALT) levels were elevated in *Atp7b*$^{-/-}$ mice and increased after BMT. (D) Serum ceruloplasmin was lower in *Atp7b*$^{-/-}$ mice with or without BMT than healthy controls. *p* Values, ANOVA, Kruskall–Wallis test.

Serum ALT in healthy C57BL/6 mice ($n=4$) was 54± 17 U/L (Fig. 1C). ALT levels in untreated *Atp7b*$^{-/-}$ mice ($n=8$) were higher (172±36 U/L, $p<0.001$). After BMT, ALT levels were higher still, after both 6 months ($n=8$) and 12 months ($n=4$), 447±127 and 214±110 U/L, respectively. Ceruloplasmin levels were lower in *Atp7b*$^{-/-}$ mice with or without BMT versus C57BL/6 controls (Fig. 1D).

Liver Fibrosis Accelerated in Atp7b$^{-/-}$ *Mice After BMT*

Untreated *Atp7b*$^{-/-}$ mice showed multiple WD-associated changes. In *Atp7b*$^{-/-}$ mice with BMT, liver histology worsened (Fig. 2A). Megalocytosis marking advanced polyploidy was prominent after BMT. Sirius Red showed more fibrosis after BMT (Fig. 2B). Histological grading after 12 months was 2±0, 6.3±0.3, and 7.9±0.3 in healthy C57BL/6 ($n=9$), untreated *Atp7b*$^{-/-}$ controls ($n=8$), and *Atp7b*$^{-/-}$ mice with BMT ($n=7$), respectively ($p<0.001$, ANOVA) (Fig. 2C). Sirius Red area in healthy controls ($n=9$) was 8.7±0.9%, rising in *Atp7b*$^{-/-}$ mice ($n=8$) and *Atp7b*$^{-/-}$ mice with BMT ($n=7$) to 31.7±2.2% and 38.3±0.9%, respectively ($p<$ 0.001, ANOVA). Hepatic hydroxyproline increased from 0.2±0.1 mg/g in C57BL/6 mice ($n = 4$) by 2.5-fold, and 4.5- and 3.5-fold in *Atp7b*$^{-/-}$ controls or mice 6 and 12 months after BMT ($n=4$ each), respectively ($p<0.001$, ANOVA) (Fig. 2D).

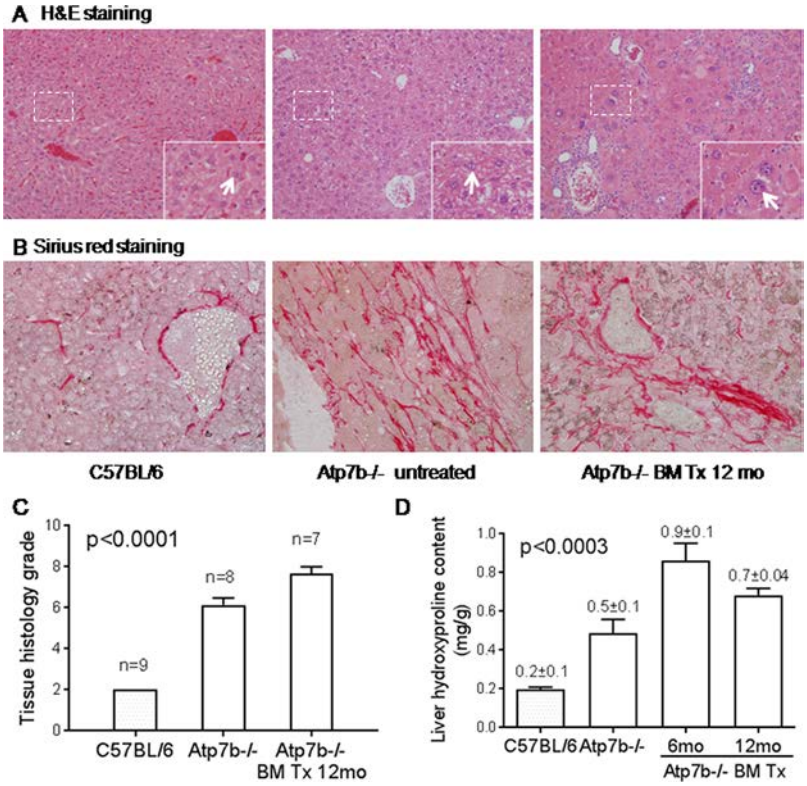

Figure 2. Liver histology after 12 months. (A) Healthy C57BL/6 mice showed normal morphology (left, inset, arrow, size of normal nuclei). Liver injury was evident in *Atp7b*$^{-/-}$ mice, including after BMT (insets: megalocytes with enlarged nuclei). (B) Sirius Red staining showed more collagen in untreated *Atp7b*$^{-/-}$ controls and *Atp7b*$^{-/-}$ mice after BMT. Original magnification: 400 . (C) Grading for tissue histology indicated worsening in *Atp7b*$^{-/-}$ mice after BMT. (D) Tissue hydroxyproline levels were higher in *Atp7b*$^{-/-}$ mice than healthy controls. These increased in mice after BMT. *p* Values, ANOVA, Kruskall–Wallis test.

Hepatic Cu Content, Atp7b *mRNA Expression, and Cell Damage*

Healthy C57BL/6 mice ($n=9$) had 0.016 ± 0.00 mg Cu/g liver after 12 months. In untreated *Atp7b*$^{-/-}$ controls ($n=8$), significantly more Cu was found (0.18 ± 0.01 mg/g, $p<0.001$). In *Atp7b*$^{-/-}$ mice with BMT, liver Cu was even higher, both after 6 months ($n=9$) and 12 months ($n=7$) (0.26 ± 0.05 and 0.38 ± 0.05 mg/g, respectively; $p<0.05$) (Fig. 3A). *Atp7b* mRNA was present in only healthy C57BL/6 mice and not in untreated *Atp7b*$^{-/-}$ or *Atp7b*$^{-/-}$ mice with BMT ($n=3$ each) (Fig. 3B). These suggested donor-derived hepatocytes did not repopulate the liver after BMT. To determine the basis for lack of proliferation in native hepatocytes, we examined oxidative DNA damage, which results from Cu toxicosis and impairs liver regeneration[24] (Fig. 3C). In healthy C57BL/6 mice, hepatic 8-oxo-dG adducts were not prominent. *Atp7b*$^{-/-}$ mice showed considerable 8-oxo-dG adducts, particularly in megalocytes or polyploid cells and also in inflammatory and stromal cells. This damage in native hepatocytes was more pronounced in *Atp7b*$^{-/-}$ mice with BMT. Losses of these cells should have led to greater compensatory proliferation in healthy donor-derived hepatocytes.

Inflammation and Fibrosis-Related Genes Were Expressed More After BMT

Genes contributing to inflammation (*IL6* and *TNF-*) and fibrogenesis (*TGF-* , *MMP2*, *TIMP1*, and *COL1*) were expressed more in *Atp7b*$^{-/-}$ mice versus healthy controls ($n=3$ each) (Fig. 4). *IL6*, *TNF-* , and *TGF-* were expressed even more in *Atp7b*$^{-/-}$ mice after BMT ($n=3$)—more after 6 versus 12 months; fibrotic tissue in latter samples could have affected gene expression. As inflammation likely recruited cell types, aggravating fibrosis, *MMP2*, *TIMP1*, and *COL1* expression profiles were in agreement with this possibility.

Replacement of Liver Cell Types by Donor BM-Derived Cells

Donor-derived GFP$^+$/Dpp4$^+$ hepatocytes were still surprisingly rare after 12 months. In *Atp7b*$^{-/-}$ mice with BMT, we observed neither proliferating donor-derived cells nor liver repopulation (Fig. 5A). GFP$^+$ donor cells were mostly in hepatic sinusoids with F4/80$^+$ monocytes or macrophages (Fig. 5B). GFP$^+$/vimentin$^+$ mesenchymal cells, including myofibroblasts, were also abundant (Fig. 5C).

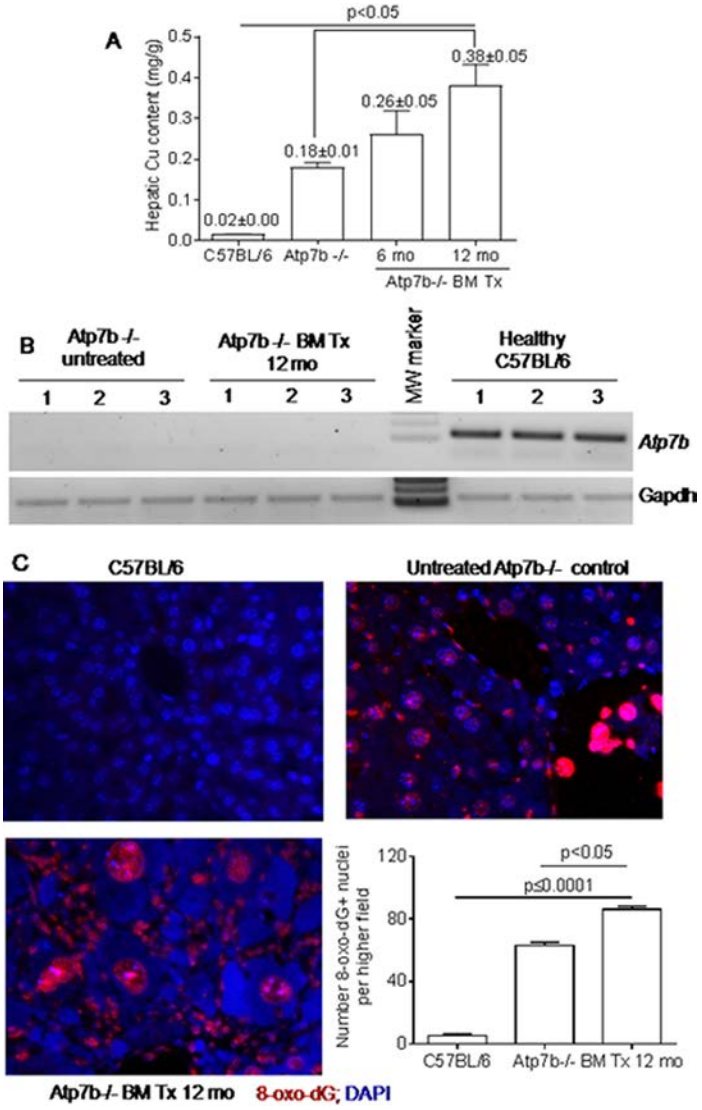

Figure 3. Hepatic Cu and *Atp7b* mRNA with changes in liver cells. (A) Compared with healthy C57BL/6 mice, liver Cu content increased in *Atp7b*$^{-/-}$ controls and *Atp7b*$^{-/-}$ mice after BMT. (B) Reverse transcription (RT)-PCR revealed *Atp7b* mRNA in healthy C57BL/6 mice, but not in either untreated *Atp7b*$^{-/-}$ mice or *Atp7b*$^{-/-}$ mice after BMT. (C) Oxidative DNA damage with 8-oxo-dG adducts in the liver (red color) of *Atp7b*$^{-/-}$ mice after 12 months, including in hepatocytes and inflammatory or stromal cells. These adducts were abundant in *Atp7b*$^{-/-}$ mice after BMT. Chart provides cumulative analysis for adducts. Original magnification: 400 . DAPI counterstain.

Morphometry indicated donor-derived cell types 12 months after BMT constituted Dpp4^{+} hepatocytes in <0.05%, F4/80^{+} monocytes/macrophages in 14%, and vimentin^{+} mesenchymal cells in 84% of the cases (Table 2).

DISCUSSION

Donor BM generated multiple cell types in *Atp7b*$^{-/-}$ mice, although hepatocytes were infrequent, which was similar to previous reports[3,20]. Extensive BM chimerism along with numerous monocytes/macrophages indicated BMT was successful. The contribution of TBI for replacing native BM is critical. Although TBI may cause early inflammation and endothelial injury [later, veno-occlusive disease (VOD)], after successful BMT, these complications abate or resolve. Long-term hepatic damage after TBI is limited; after 1 year, mice exhibit only mitosis[25]. Alternatively, BMT may use drug myeloablation (e.g., busulfan and cyclophosphamide)[26]. However, VOD may actually be more severe with these drugs, as opposed to TBI. That was not the case in our study.

In pluripotent stem cells, hepatic differentiation is restricted, at best, to early stage fetal hepatocytes in vitro[9,27]. Stem cell differentiation is aided by additional

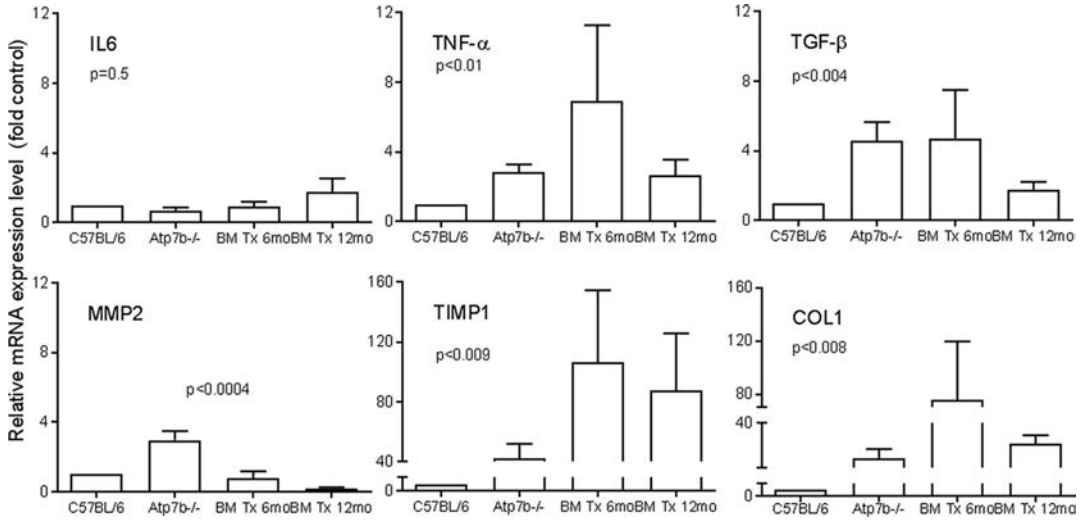

Figure 4. Quantitative RT-PCR for inflammatory and fibrogenic genes. Gene expression normalized to *Gapdh* in C57BL/6 and *Atp7b*$^{-/-}$ control mice and *Atp7b*$^{-/-}$ mice 6 or 12 months after BMT. *IL6* and *TNF-* were expressed more after BMT. Similarly, *TGF-* , *TIMP1*, and *collagen1* were expressed more, but *MMP2* was expressed less after BMT, indicating fibrogenesis-associated processes. These changes were more pronounced at 6 months after BMT. Whether more fibrosis at later times introduced sampling issues was not excluded. *p* Values, ANOVA, Kruskall–Wallis test.

signals and cues in vivo. This differentiation is achieved by incompletely understood and complex mechanisms, including transcription factor regulation, protein–protein interactions, RNA–protein changes, DNA methylation, epigenetic reprogramming, etc.[27]. These mechanisms are difficult, if not impossible, to decipher in rare donor-derived cells in vivo.

Presence of Dpp4^{+} bile canaliculi in BM-derived hepatocytes indicated maturity[10,11]. To date, no study has utilized this stringent marker in WD of Dpp4^{+} bile canaliculi for

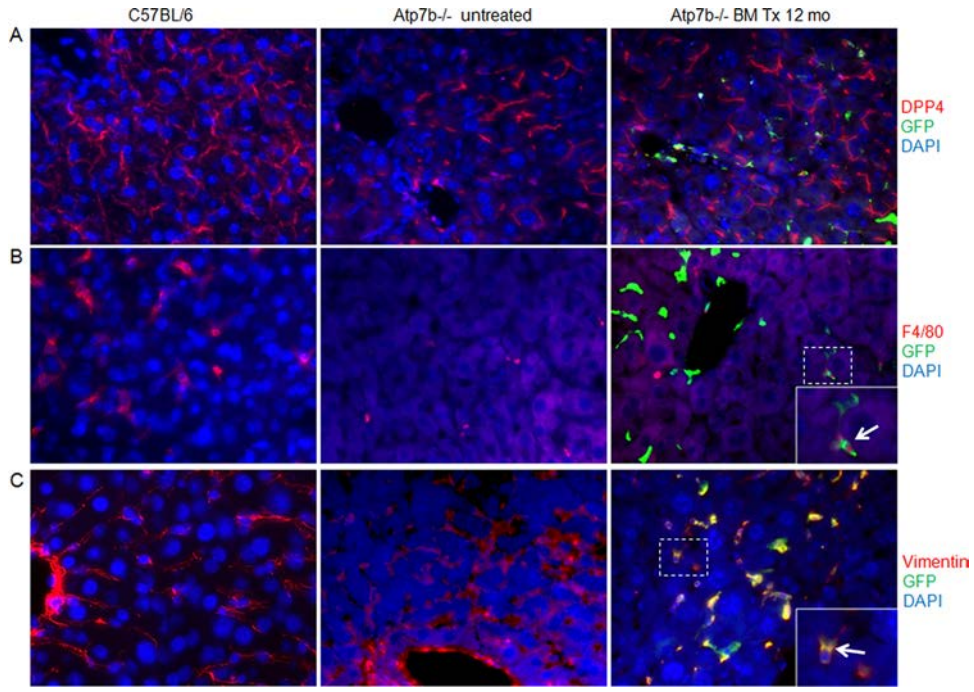

Figure 5. Donor BM-derived cell types in liver after 12 months. (A) GFP and Dpp4 staining for bile canaliculi (red color) in hepatocytes. GFP^{+}/Dpp4^{+} cells did not expand or form clusters after BMT. (B) F4/80 (red) in donor-derived monocytes/macrophages (inset: arrow, GFP^{+}/F4/80^{+} cell in sinusoid). (C) Costaining for vimentin (red) with green/yellow donor-derived myofibroblasts throughout the liver (inset: arrow, donor-derived myofibroblast). Original magnification: 400 . DAPI counterstain.

Table 2. Morphometry for Donor-Derived Cells in Liver of *Atp7b*$^{-/-}$ Mice 1 Year After Bone Marrow Transplant

Donor-Derived Cell Type	No. of GFP$^+$ Donor BM Cells per High Power Field [Mean ± SEM (*n*)]*	No. of GFP$^+$/Hepatic Marker$^+$ Donor BM-Derived Cells per High Power Field*	Percent of GFP$^+$ Cells (Mean)	*p* Values (ANOVA)†
Hepatocytes with Dpp4$^+$ bile canaliculi	136 ± 2 (*n* = 61)	0.05 ± 0.0	0.04	–
F4/80$^+$ Kupffer cells and monocytes	142 ± 2 (*n* = 40)	20 ± 1	14	<0.001
Vimentin$^+$ mesenchymal cells	154 ± 2 (*n* = 47)	129 ± 2	84	<0.001

*Cell numbers were multiplied by a factor of 2 because 50% of GFP$^{+/-}$ transgenic donor cells expressed GFP.
†*p* Values versus percent of GFP$^+$ hepatocytes.

stem cell-derived hepatocytes. This structure-based analysis should be significant, as gene expression alone to characterize cell maturity has often been inadequate[6,8,9]. Lack of hepatic *Atp7b* mRNA and continued Cu accumulation after BMT were prominent in our study. Histological abnormalities also worsened after BMT. This differed from toxic milk mouse model of Cu toxicosis, where transplantation of healthy BM in sublethally irradiated recipients decreased hepatic Cu[28]. The fate of transplanted BM-derived cells in that study was not evaluated. Also, it was unknown whether Cu was excreted in bile.

Proliferation restriction in BM-derived hepatocytes was another issue for therapeutic benefits. Inability of BM-derived hepatocytes to correct disease in *Atp7b*$^{-/-}$ mice concerned two major processes: 1) donor BM-derived hepatocytes with bile canaliculi were uncommon, and 2) proliferation in BM-derived hepatocytes was restricted. Antiproliferative effects of Cu, potential growth factor deficiencies, ECM alterations, inflammation, or other changes were likely contributors.

A major difference in animal models of WD (*Atp7b*$^{-/-}$ mice) versus tyrosinemia (*Fah*$^{-/-}$ mice) is that Cu toxicosis causes intracellular injury plus extracellular perturbations due to tissue inflammation, fibrosis, and ECM changes[14,15]. In the *Fah*$^{-/-}$ state, toxic tyrosine metabolites are restricted to hepatocytes without such inflammation or fibrosis[29]. Similar considerations apply to mice with mutant -1 antitrypsin and intracellular injury[12]. We did not focus on whether BM-derived cells fused with native hepatocytes, as in *Fah*$^{-/-}$ mice[30]. This cell fusion had not interfered with disease correction[3].

In the LEC rat model of WD, transplanted hepatocytes repopulate the liver, and hepatic radiation or other pro-oxidant treatments, in fact, accelerate proliferation in transplanted hepatocytes[14,15]. Similarly, healthy hepatocytes proliferated in *Atp7b*$^{-/-}$ mice. As Cu alters ECM to impair cell survival and/or proliferation[31], this might have affected donor-derived hepatocytes. Remote TBI should not have directly injured donor-derived hepatocytes. Hepatic radiation in excess of that after TBI did not exacerbate fibrosis in LEC rats[14,15].

Tissue inflammation triggers multiple cytokine-, chemokine-, and receptor-mediated events driving fibrogenesis. The GFP$^+$/F4/80$^+$ macrophages/monocytes and GFP$^+$/vimentin$^+$ mesenchymal cells in *Atp7b*$^{-/-}$ mice after BMT should have contributed to inflammatory cytokines and fibrogenesis. Inflammatory cytokines and chemokines, including TNF- and IL6, from activated neutrophils and KC impair hepatocyte survival and liver repopulation[32,33]. Previous studies of hepatic stellate cells (HSCs) indicated that these play important roles in ECM remodeling during cell engraftment in the liver[34]. HSCs release deleterious cytokines during fibrogenesis (e.g., TGF- , to suppress hepatocyte proliferation)[35]. This might have affected proliferation in donor-derived cells in WD. Activation of HSC promotes expansion of myofibroblasts, which was reproduced by donor BM-derived cells in hepatic fibrosis[36]. Similarly, exposure of transplanted HSC to fibrogenic injuries in the liver led to their conversion into myofibroblasts, along with recruitment of monocytes and KC to further exacerbate hepatic fibrosis[37]. Targeting of donor-derived myofibroblasts involves ligand–receptor interactions (e.g., cannabinoid receptors)[38]. Altered expression of matrix degrading enzymes (MMP and TIMP) and of collagen in *Atp7b*$^{-/-}$ mice after BMT was in agreement with the contribution of inflammatory cell types in hepatic fibrosis.

Stem cell transplantation is of interest for chronic liver disease[7], although trials of hematopoietic or mesenchymal stem cells (MSCs) have not shown clear benefits[39]. In one animal study, BM-derived healthy MSCs expressing *Atp7b*[40] improved their survival and proliferation. In another study, transplantation of *Atp7b*-transduced MSCs in LEC rats[41] decreased liver Cu over the short term. Our work in *Atp7b*$^{-/-}$ mice indicates analysis of candidate stem cells in representative settings will be helpful for clinical trials.

ACKNOWLEDGMENTS: This work was supported in part by NIH grants R01-DK071111, P30-DK41296, P30-CA013330, and P30 DK020541, and by the New York State Department of Health/NYSTEM Shared Facilities program (contract C029154). Gertrude Ukpong contributed technical expertise. The authors declare no conflicts of interest.

REFERENCES

1. Viswanathan P, Gupta P, Kapoor S, Gupta S. Thalidomide promotes transplanted cell engraftment in the rat liver by modulating inflammation and endothelial integrity. J Hepatol. 2016;65(6):1171–8.
2. Yovchev MI, Xue Y, Shafritz DA, Locker J, Oertel M. Repopulation of the fibrotic/cirrhotic rat liver by transplanted hepatic stem/progenitor cells and mature hepatocytes. Hepatology 2014;59(1):284–95.
3. Lagasse E, Connors H, Al-Dhalimy M, Reitsma M, Dohse M, Osborne L, Wang X, Finegold M, Weissman IL, Grompe M. Purified hematopoietic stem cells can differentiate into hepatocytes in vivo. Nat Med. 2000;6(11):1229–34.
4. Grompe M, Strom S. Mice with human livers. Gastroenterology 2013;145(6):1209–14.
5. Roobrouck VD, Clavel C, Jacobs SA, Ulloa-Montoya F, Crippa S, Sohni A, Roberts SJ, Luyten FP, Van Gool SW, Sampaolesi M, and others. Differentiation potential of human postnatal mesenchymal stem cells, mesoangioblasts, and multipotent adult progenitor cells reflected in their transcriptome and partially influenced by the culture conditions. Stem Cells 2011;29(5):871–82.
6. Espejel S, Eckardt S, Harbell J, Roll GR, McLaughlin KJ, Willenbring H. Brief report: Parthenogenetic embryonic stem cells are an effective cell source for therapeutic liver repopulation. Stem Cells 2014;32(7):1983–8.
7. Forbes SJ, Gupta S, Dhawan A. Cell therapy for liver disease: From liver transplantation to cell factory. J Hepatol. 2015;62(1 Suppl):S157–69.
8. Zhu S, Rezvani M, Harbell J, Mattis AN, Wolfe AR, Benet LZ, Willenbring H, Ding S. Mouse liver repopulation with hepatocytes generated from human fibroblasts. Nature 2014;508(7494):93–7.
9. Bandi S, Cheng K, Joseph B, Gupta S. Spontaneous origin from human embryonic stem cells of liver cells displaying conjoint meso-endodermal phenotype with hepatic functions. J Cell Sci. 2012;125(Pt 5):1274–83.
10. Gupta S, Rajvanshi P, Lee CD. Integration of transplanted hepatocytes into host liver plates demonstrated with dipeptidyl peptidase IV-deficient rats. Proc Natl Acad Sci USA 1995;92(13):5860–4.
11. Gupta S, Rajvanshi P, Sokhi R, Slehria S, Yam A, Kerr A, Novikoff PM. Entry and integration of transplanted hepatocytes in rat liver plates occur by disruption of hepatic sinusoidal endothelium. Hepatology 1999;29(2):509–19.
12. Baligar P, Kochat V, Arindkar SK, Equbal Z, Mukherjee S, Patel S, Nagarajan P, Mohanty S, Teckman JH, Mukhopadhyay A. Bone marrow stem cell therapy partially ameliorates pathological consequences in livers of mice expressing mutant human alpha1-antitrypsin. Hepatology 2017;65(4):1319–35.
13. Schilsky ML. A century for progress in the diagnosis of Wilson disease. J Trace Elem Med Biol. 2014;28(4): 492–4.
14. Malhi H, Joseph B, Schilsky ML, Gupta S. Development of cell therapy strategies to overcome copper toxicity in the LEC rat model of Wilson disease. Regen Med. 2008;3(2):165–73.
15. Joseph B, Kapoor S, Schilsky ML, Gupta S. Bile salt-induced pro-oxidant liver damage promotes transplanted cell proliferation for correcting Wilson disease in the Long-Evans Cinnamon rat model. Hepatology 2009;49(5):1616–24.
16. Murillo O, Luqui DM, Gazquez C, Martinez-Espartosa D, Navarro-Blasco I, Monreal JI, Guembe L, Moreno-Cermeno A, Corrales FJ, Prieto J, and others. Long-term metabolic correction of Wilson's disease in a murine model by gene therapy. J Hepatol. 2016;64(2):419–26.
17. Gupta S. Cell therapy to remove excess copper in Wilson's disease. Ann NY Acad Sci. 2014;1315:70–80.
18. Lutsenko S. Atp7b-/- mice as a model for studies of Wilson's disease. Biochem Soc Trans. 2008;36(Pt 6):1233–8.
19. Merlin S, Bhargava KK, Ranaldo G, Zanolini D, Palestro CJ, Santambrogio L, Prat M, Follenzi A, Gupta S. Kupffer cell transplantation in mice for elucidating monocyte/macrophage biology and for potential in cell or gene therapy. Am J Pathol. 2016;186(3):539–51.
20. Follenzi A, Raut S, Merlin S, Sarkar R, Gupta S. Role of bone marrow transplantation for correcting hemophilia A in mice. Blood 2012;119(23):5532–42.
21. Jaber FL, Sharma Y, Gupta S. Demonstrating potential of cell therapy for Wilson's disease with the Long-Evans cinnamon rat model. Methods Mol Biol. 2017;1506:161–78.
22. Malhi H, Bhargava KK, Afriyie MO, Volenberg I, Schilsky ML, Palestro CJ, Gupta S. 99mTc-mebrofenin scintigraphy for evaluating liver disease in a rat model of Wilson's disease. J Nucl Med. 2002;43(2):246–52.
23. Evenson MA. Measurement of copper in biological samples by flame or electrothermal atomic absorption spectrometry. Methods Enzymol. 1988;158:351–7.
24. Gorla GR, Malhi H, Gupta S. Polyploidy associated with oxidative injury attenuates proliferative potential of cells. J Cell Sci. 2001;114(Pt 16):2943–51.
25. Travis EL, Peters LJ, McNeill J, Thames HD Jr, Karolis C. Effect of dose-rate on total body irradiation: Lethality and pathologic findings. Radiother Oncol. 1985;4(4):341–51.
26. Qiao J, Fu J, Fang T, Huang Y, Mi H, Yang N, Chen C, Xu K, Zeng L. Evaluation of the effects of preconditioning regimens on hepatic veno-occlusive disease in mice after hematopoietic stem cell transplantation. Exp Mol Pathol. 2015;98(1):73–8.
27. Bandi S, Gupta S, Tchaikovskaya T, Gupta S. Differentiation in stem/progenitor cells along fetal or adult hepatic stages requires transcriptional regulators independently of oscillations in microRNA expression. Exp Cell Res. 2018; 370(1):1–12.
28. Allen KJ, Cheah DM, Lee XL, Pettigrew-Buck NE, Vadolas J, Mercer JF, Ioannou PA, Williamson R. The potential of bone marrow stem cells to correct liver dysfunction in a mouse model of Wilson's disease. Cell Transplant. 2004;13(7):765–73.
29. Vogel A, Aslan JE, Willenbring H, Klein C, Finegold M, Mount H, Thomas G, Grompe M. Sustained phosphorylation of Bid is a marker for resistance to Fas-induced apoptosis during chronic liver diseases. Gastroenterology 2006;130(1):104–19.
30. Vassilopoulos G, Wang PR, Russell DW. Transplanted bone marrow regenerates liver by cell fusion. Nature 2003; 422(6934):901–4.
31. Giri RK, Malhi H, Joseph B, Kandimalla J, Gupta S. Metal-catalyzed oxidation of extracellular matrix components perturbs hepatocyte survival with activation of intracellular signaling pathways. Exp Cell Res. 2003;291(2):451–62.
32. Krohn N, Kapoor S, Enami Y, Follenzi A, Bandi S, Joseph B, Gupta S. Hepatocyte transplantation-induced liver inflammation is driven by cytokines-chemokines

associated with neutrophils and Kupffer cells. Gastroenterology 2009;136(5):1806–17.
33. Viswanathan P, Kapoor S, Kumaran V, Joseph B, Gupta S. Etanercept blocks inflammatory responses orchestrated by TNF-alpha to promote transplanted cell engraftment and proliferation in rat liver. Hepatology 2014;60(4):1378–88.
34. Benten D, Kumaran V, Joseph B, Schattenberg J, Popov Y, Schuppan D, Gupta S. Hepatocyte transplantation activates hepatic stellate cells with beneficial modulation of cell engraftment in the rat. Hepatology 2005;42(5):1072–81.
35. Dixon M, Agius L, Yeaman SJ, Day CP. Inhibition of rat hepatocyte proliferation by transforming growth factor beta and glucagon is associated with inhibition of ERK2 and p70 S6 kinase. Hepatology 1999;29(5):1418–24.
36. Forbes SJ, Russo FP, Rey V, Burra P, Rugge M, Wright NA, Alison MR. A significant proportion of myofibroblasts are of bone marrow origin in human liver fibrosis. Gastroenterology 2004;126(4):955–63.
37. Benten D, Kluwe J, Wirth JW, Thiele ND, Follenzi A, Bhargava KK, Palestro CJ, Koepke M, Tjandra R, Volz T, Lutgehetmann M, Gupta S. A humanized mouse model with liver fibrosis following expansion of transplanted hepatic stellate cells in injury and inflammation. Lab Invest. 2018; 98:525–36.
38. Wang L, Yang L, Tian L, Mai P, Jia S, Yang L, Li L. Cannabinoid receptor 1 mediates homing of bone marrow-derived mesenchymal stem cells triggered by chronic liver injury. J Cell Physiol. 2017;232(1):110–21.
39. Nicolas CT, Wang Y, Nyberg SL. Cell therapy in chronic liver disease. Curr Opin Gastroenterol. 2016;32(3):189–94.
40. Sauer V, Siaj R, Todorov T, Zibert A, Schmidt HH. Overexpressed ATP7B protects mesenchymal stem cells from toxic copper. Biochem Biophys Res Commun. 2010;395(3): 307–11.
41. Chen S, Shao C, Dong T, Chai H, Xiong X, Sun D, Zhang L, Yu Y, Wang P, Cheng F. Transplantation of ATP7B-transduced bone marrow mesenchymal stem cells decreases copper overload in rats. PLoS One 2014;9(11):e111425.